AENSI Journals

Australian Journal of Basic and Applied Sciences

ISSN:1991-8178

Journal home page: www.ajbasweb.com

A Hybrid Maximum Likelihood Estimation Approach for non-local medical image denoising and tumour detection using Cuckoo-based Neuro Fuzzy Classifiers

[1]A. Velayudham, [2]Dr.R. Kanthavel, [3]K. Madhan Kumar

[1]*Assistant Professor (SG), Department of IT, Cape Institute of Technology, Levengipuram-627114, Tirunelveli District, India.*
[2]*Professor and Head, Department of ECE, Velammal Engineering College, Chennai-66, India.*
[3]*Associate Professor, Department of ECE, PET Engineering College, Vallioor-627117, Tirunelveli District, India.*

ARTICLE INFO

Article history:
Received 10 October 2014
Received in revised form
22 November 2014
Accepted 28 November 2014
Available online 1 December 2014

Keywords:
PSNR, SDME, CNF, Contrast, Energy, Entropy, K-means, Sensitivity, Specificity, Accuracy, Maximum Likelihood

ABSTRACT

Medical images are usually corrupted by several noises starting right from the acquiring process complicating the automatic feature extraction and analysis of clinical data. To obtain the best possible diagnosis it is vital that medical images be clear, sharp, and free of noise and artifacts. In this research paper, we propose a hybrid method to denoise, detect and classify the tumour part from CT medical images. Our proposed approach consists of four phases, such as denoising, region segmentation, feature extraction and classification. In the denoising phase Maximum Likelihood estimation method is being used for removing noise. We have taken into consideration two noises, Gaussian and salt & pepper for the proposed technique. The performance of the proposed technique is assessed on the five CT images for the parameters, PSNR and SDME. In the segmentation process K-means clustering technique is employed. For the feature extraction, the parameters contrast, energy and gain are extracted. In classification, a modified technique called Cuckoo-Neuro Fuzzy (CNF) algorithm is developed and applied for detection of the tumour region. Then, classification is done based on the fuzzy rules generated. The proposed denoising technique have shown better values for the SDME of 69.8798 and PSNR of 25.1008 for salt & pepper noise which is very superior compared to existing methods. Moreover it has shown an accuracy of 96.9%. The obtained results have been found to be better than the existing methods.

To Cite This Article: A. Velayudham, R. Kanthavel and K. Madhan Kumar., A Hybrid Maximum Likelihood Estimation Approach for non-local medical image denoising and tumour detection using Cuckoo-based Neuro Fuzzy Classifiers. ***Aust. J. Basic & Appl. Sci.,*** *8(18): 335-349, 2014*

INTRODUCTION

Denoising of medical images like X-RAY, CT, MRI, PET and SPECT encompass diminutive information about heart, brain, nerves and more which leads physician for precise analysis of diseases (Naga Prudhvi Raj V., 2012). In the case of CT, numerous mathematical and medical applications can be applied to conclude whether the normal tissue has been infected by the mutations of the cancer cell (Shanshan Wang, 2012; Ehsan Nadernejad, 2012). Recent wavelet thresholding based denoising methods have proved capable, during the conservation of the high frequency signal details (Anja Borsdorf, 2008). The threshold at certain scale is a constant for all wavelet coefficients in standard wavelet thresholding based noise reduction methods (Abdolhossein Fathi, 2012). Fundamentally, the noisy image is transformed into the wavelet domain, then the wavelet coefficients are shifted to soft or hard thresholding, and the result has been inverse-transformed in the final step (Sudipta Roy, 2010; Shutao Li, 2012). Medical image segmentation casts an amazing part in the treatment planning, identifying tumours, tumour volume, patient follow up and computer guided surgery. There is a flood of varied methods for performing the function of medical image segmentation (Minakshi Sharma, 2012).

In this study, a new denoising method based on Maximum Likelihood (ML) estimation methods were proved to be very effective in denoising medical images along with spectral subtraction of the measured noise power from each signal acquisition is presented (Savitharaj, N.S., 2014; Arcan Erturk, M., 2013). The Proposed approach is an adaptive non local ML estimation method for denoising medical images in which the samples are selected in an adaptive way for the ML estimation of the true underlying signal. In this, we introduce a new, time efficient, image denoising method by applying maximum likelihood method directly to medical image acquisitions in k-space. Maximum likelihood method is simple and capable to handle dense noise image. This

Corresponding Author: A.Velayudham, Assistant Professor (SG), Department of Information Technology, Cape Institute of Technology, Levengipuram – 627114, Tirunelveli District, India.
E-mail: a.velayudham@gmail.com

method is capable to denoise multiple-coil acquired medical images. Both the non-central distribution and the spatially varying nature of the noise are taken into account in the proposed method.

Feature extraction is the task of mining definite features from the pre-processed image. Nowadays, many diverse methods are employed for estimating texture like co-occurrence matrix, Fractals, Gabor filters, wavelet transform. Gray Level Co-occurrence Matrix (GLCM) features are extensively utilized to break-up regular and irregular brain tumours (Minakshi Sharma, 2012; Jitendra Malik, 2001). K-means clustering is an appropriate method for biomedical image segmentation as the quantity of clusters is generally identified for images of particular regions of the human anatomy. A number of experimenters have launched associated investigations into K-means clustering segmentation. Though a significant and noteworthy advancement has been made in this regard, still there is greater computational intricacy and the need for superfluous software functionality (Rakesh M., 2012). Clustering programs, like k-means and ISODATA, function in an unsupervised mode and have been performed on an extensive domain of categorization dilemmas (Kekre, H.B., 2010). For categorizing the tumour segments, physical classification tends to lead to manual flaws, in addition to relying heavily on person to person, protracted and elongated runtime along with non-reproducible outcomes. Therefore, an automatic or semi-automatic classification technique is the need of the hour as it tends to scale down the burden on the individual spectator, and also because accuracy does not become the casualty on account of exhaustion and mammoth quantity of images (Minakshi Sharma, 2012). In respect of tumour detection, several schemes such as, K-NN, bayesian classifier, neural network, fuzzy classifier are performed for automatic detection. When comparing with these methods, Neuro-Fuzzy is found to be better and this technique has been used in a lot of research areas.

2. Existing Approaches:

A few of the modern related works concerning the denoising and classification are reviewed in this section. A. Velayudham *et al.,* (2013) have proposed an efficient technique to denoise CT images using Dual Tree Complex Wavelet Packet Transform and Empirical Mode Decomposition. O. Tischenko *et al.,* (2005) have presented a structure-saving noise minimizing technique using the correlations between two images for calculation of threshold in the wavelet domain. In addition, Anja Borsdorf *et al.*, (2008) by discovering a method to obtain spatially identical input images in case of CT have reduced the problems that occur in this technique. G.Y. Chen and B.Kegl (2005) devised an image denoising method by incorporating the dual-tree complex wavelets into the ordinary ridgelet transform. Joao M. Sanches *et al.,* (2008) have examined and presented a bayesian denoising algorithm which copes with additive white Gaussian and multiplicative noise described by Poisson and Rayleigh distributions. Faten Ben Arfia *et al.*, (2010) have developed a method for image denoising in the filter domain based on the characteristics of the Empirical Mode Decomposition (EMD) and the wavelet technique. Guangming Zhang *et al.*, have developed a model for CT medical image de-noising, which was using independent component analysis and curvelet transform. Syed Amjad Ali *et al.,* (2010) have forecasted an efficient noise reduction technique for CT images using window-based Multi-wavelet transformation and thresholding. G. Landi and E. Loli Piccolomini *et al.,* (2012) have modeled a denoising problem in a Bayesian statistical setting by a non-negatively constrained minimization problem.

Jue Wu and Albert C.S Chung (2009) stated a template-based framework and Markov dependence tree method for segmentation which were used to segment the deep brain structure. Also, a methodology has been developed using vector flow method to overcome the gradient vector flow, boundary vector flow, and magneto static active contour, but it has the limited range only (Qin A.K and David A. Clausi, 2010; Tao Wang *et al.*, 2009). On other hand, Zafer Iscan *et al.*, (2010) have given a technique for segmenting the tumors in medical images. There, tumour identifications were done by 2D Continuous wavelet transform. Reza Farjam *et al.*, (2012) have designed an approach to localize small metastatic lesions. The key problem in medical imaging was automatically segmenting an image into constituent heterogeneous process. Rakesh, M. and T. Ravi (2012) have presented a segmentation technique using fuzzy C-means algorithm. The segmentation performed only at an average speed in their method. Minakshi Sharma and Dr. Sourabh Mukharjee (2012) have formulated an approach for segmenting the brain tumor using Adaptive Neuro-Fuzzy Inference System (ANFIS) to overcome the speed factor of the fuzzy C-means algorithm.

In Wavelet-Based Rician Noise Removal for Magnetic Resonance Imaging, the filtering methods for Rician noise removal has been explained and a novel wavelet-domain filter that adapts to variations in both the signal and the noise has been presented (Nowak R.D., 1999). This method provides a simple and effective approach. It reduces the image contrast and it takes low computation. The major drawback in this method is it takes complex program logic for difficult system. Methodologies to denoise magnitude magnetic resonance (MR) images, which are Rician distributed has also been devised (Jeny Rajan *et al.*, 2011; Jeny Rajan *et al.*, 2012; Sijbers J. *et al.*, 1998). This method estimates the true, underlying signal from a local neighborhood within which the signal is assumed to be constant. The filtering in this approach produces blurred edges and loss of fine structures for the input image. To solve this problem they proposed a concept of restricted local neighborhoods where the true intensity for each noisy pixel is estimated from a set of preselected neighboring pixels. P. Perona and J.Malik

(1990) introduced a class of algorithms that realize anisotropic diffusion and can be applied with success to multiscale image segmentation. Anisotropic Diffusion preserves the edge junctions and the speed of computation is highly perfect. The major drawback of this paper is that the level of Noise varies significantly making the system insufficient to obtain a correct multiscale segmentation. Moreover, anisotropic diffusion can reduce the amount of work. A. Buades *et al.*, (2005) have analyzed the performance of various digital image denoising methods and evaluated them. In this paper denoising is achieved by averaging all pixels in the image. The major advantage this approach is that it will remove the noise clearly and recover the true images. Its limitation is that a small mean square error does not assure a high visual quality. G. Gerig *et al.*, (1992) have presented a research work based on Anisotropic Diffusion. The major advantage of this method is that it overcomes the blurring of object boundaries and also it increases the signal and reduces the source of noise. The major drawback of this method is inefficiency and loss of resolution.

The rest of the paper is organized as follows: an introduction of the proposed technique is presented in Section 1. The literature works of the existing approaches are presented in Section 2. The proposed CT image denoising and classification technique is detailed in Section 3. The implementation methodology is figured and given in Section 4. The obtained results are discussed in Section 5. Finally, the conclusions are summed up in Section 6.

3. Proposed Method:

The main contribution of the proposed technique is to employ Maximum Estimation Likelihood approach to denoise the image. Then segmentation process is carried out with K-means clustering. For the feature extraction, the parameters contrast, energy and gain are extracted. In classification, a modified technique called Cuckoo-Neuro Fuzzy (CNF) algorithm is developed and applied for detection of the tumour region. The overall diagram of the proposed technique is given in Figure 1.

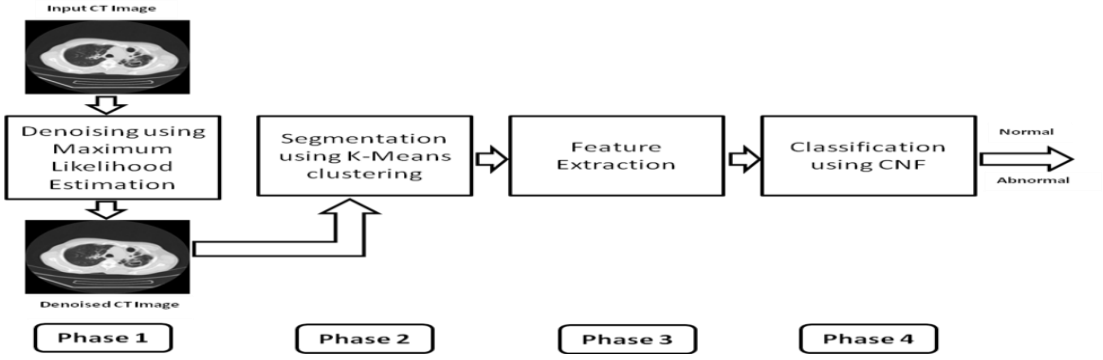

Fig. 1: Data flow diagram of the Proposed Method

- Phase 1: Denoising

Here Maximum Likelihood estimation approach is employed to remove noise from the medical CT images.

- Phase 2: Segmentation

The second phase detects the region of CT images using K-means clustering algorithm.

- Phase 3: Feature extraction

In this phase, feature parameters such as contrast, energy and gain are extracted using the segmented regions.

- Phase 4: Classification

Finally, a Cuckoo-Neuro Fuzzy algorithm is developed and used for detection of the tumour region.

3.1 Denoising Phase:

The proposed approach is an adaptive non local ML estimation method for denoising medical images in which the samples are selected in an adaptive way for the ML estimation of the true underlying signal. During acquisition process some time the k-space is sub-sampled to increase the acquisition speed, noise becomes spatially varying. The proposed method is capable to denoise multiple-coil acquired medical images. Both the non-central distribution and the spatially varying nature of the noise are taken into account. The denoising process of phase is as shown in Figure 2.

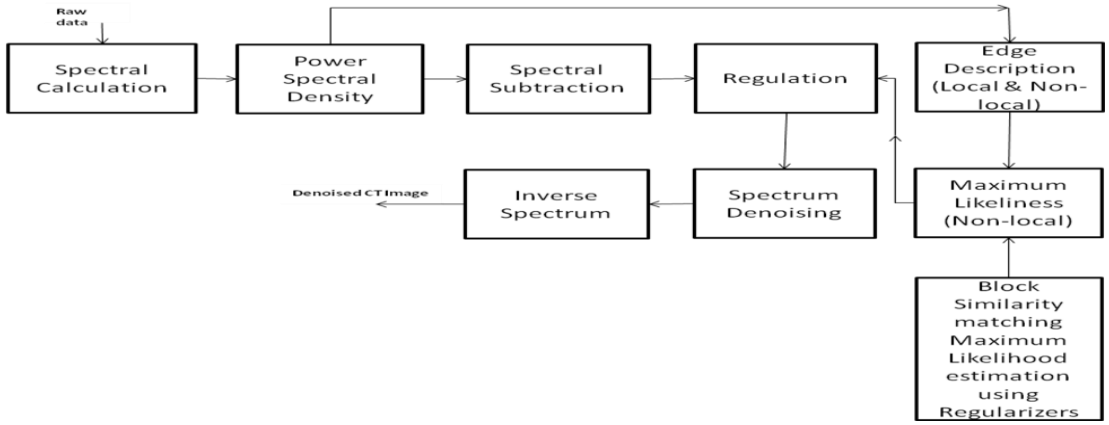

Fig. 2: Data flow diagram of the Maximum Likelihood Estimation Approach

3.1.1 Dicom Reader:

Digital Imaging and Communications in Medicine (DICOM) is a tool for handling, printing, storing and transmitting data in medical imaging. It involves a file format definition and a network communication protocol. DICOM has been widely adopted by hospitals in medical imaging applications. Figure 3 shows the working principle of Dicom Reader.

Fig. 3: Dicom Reader

3.1.2 Preprocessing:

In this sub-module, image is analyzed and preprocessing is employed that include image information calculation such as size, resolution and other aspects of the image that can be used for processing. The input image presents a set of weak features which need to be strengthened so that features can be extracted more accurately. The preprocessing technique used in this paper first converts the raw data into gray scale image based on the parameter such as resolution, size and so on. And it processes the gray scale image and produces the result. The preprocessing technique is shown in Figure 4.

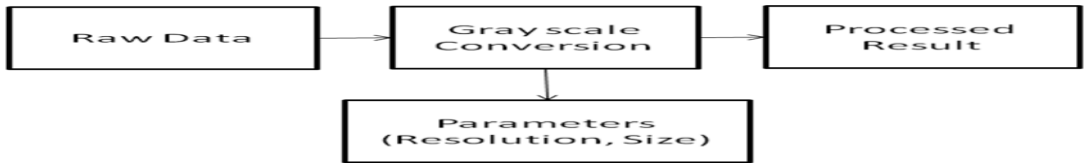

Fig. 4: Preprocessing

3.1.3 Spectral Transform:

The preprocessed result is transformed based on threshold based classification and produces the transformed result as shown in Figure 5.

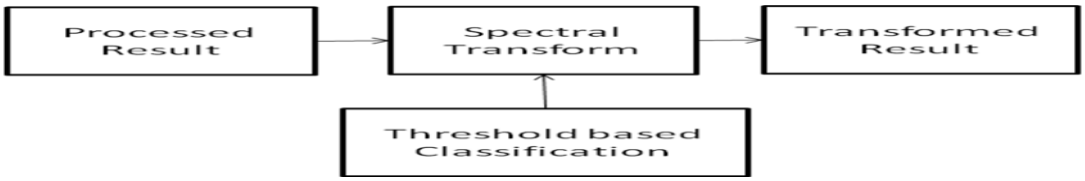

Fig. 5: Spectral Transform

The spectral transform method is based on a dual representation of the scalar fields in terms of a truncated series of spherical harmonic functions and in terms of values on a rectangular tensor-product grid whose axes represent longitude and latitude. The representation of state variables in spectral space are the coefficients of an expansion in terms of complex exponentials and associated Legendre functions, as represented in the following equation,

$$\xi(\lambda,\mu) = \sum_{m=-M}^{M} \sum_{n=|m|}^{N(m)} \xi_n^m \, P_n^m(\mu) e^{i m \lambda} \quad (1)$$

Where, the associated Legendre function and the spectral coefficients are determined by the following equations.

$$\xi_n^m = \int_{-1}^{1} \left[\frac{1}{2\Pi} \int_0^{2\Pi} \xi(\lambda,\mu) \, e^{-i m \lambda} d\lambda \right] P_n^m(\mu) d\mu \quad (2)$$

$$\xi_n^m \equiv \int_{-1}^{1} \xi^m(\mu) P_n^m(\mu) d\mu \quad (3)$$

3.1.4 Spectral Density Mapping

Spectral density mapping includes the mapping of original information based on the available density. The higher dense information is processed as a group so that the relativeness among the system can be easily grouped and the variational approach can be easily processed as shown in Figure 6.

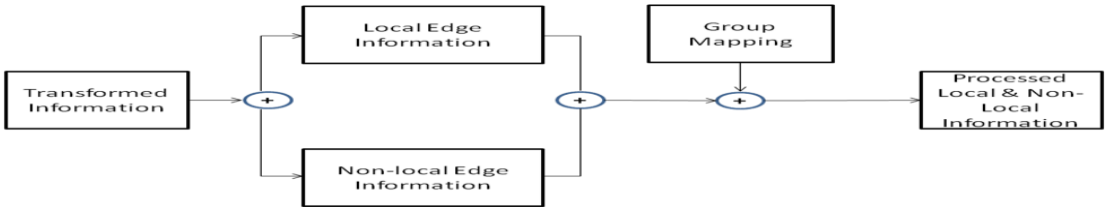

Fig. 6: Spectral Density Mapping Process

3.1.4.1 Local Information:

Local spectral analysis of images via the two-dimensional continuous wave transformation is employed to trace the local structural based data of the system.

3.1.4.2 Non-local Information:

Non-local spectral analysis of images via the two-dimensional continuous wavelet transform is employed to track the local texture based information of the system that can be mapped to increase the overall performance of the system (J. Orchard *et al.*, 2008; J.V Manjon *et al.*, 2010).

3.1.5 Spectral Subtraction:

3.1.5.1 Maximum Likelihood Estimation:

The true underlying intensity for each pixel is estimated using the ML estimation method and is applied on a set of non local (NL) pixels selected based on the intensity similarity of the pixel neighborhood. The number of NL pixels to be considered for ML estimation is fixed and is generally determined in a heuristic way. This fixed sample size can introduce under or over smoothing in the images.

3.1.5.2 Adaptive Variance Identifier:

This step is based on the threshold information. In this grouped data gets mapped into similar and non-similar structure and identifies the non-similar data for the input image. Figure 7 shows the spectral subtraction process using Maximum Likelihood (ML) Estimation Approach.

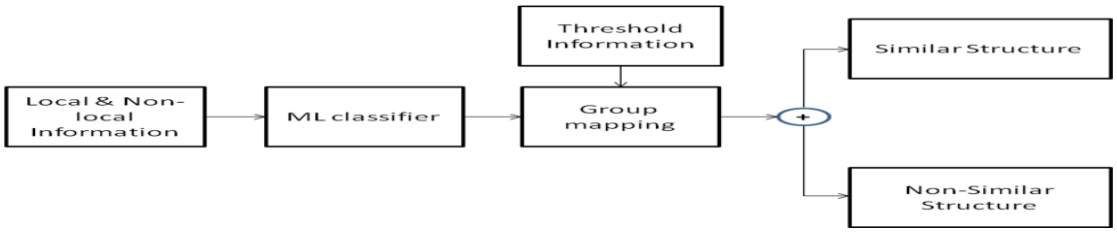

Fig. 7: Spectral Subtraction Process using ML approach

3.1.6 K-space Density Regularizer:

The acquired complex signal fills k-space matrix. Each k-space row can be modeled as an underlying true signal plus Gaussian noise.

$$x_r(t) + ix_i(t) = s_r(t) + n_r(t) + i[s_i(t) + n_i(t)] \quad (4)$$

Where x(t)is the observed k-space signal, s(t)is the true underlying noiseless k-space signal, n(t)is the noise quotient and subscripts r and i are denoted as real and imaginary components respectively. The non-similar data are grouped by similar data as represented in Figure 8.

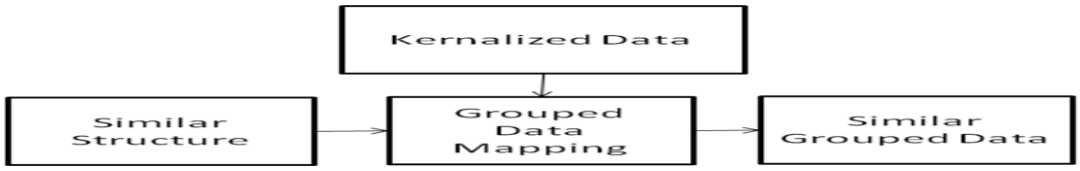

Fig. 8: K-space Density Regularizer

3.1.7 Spectral De-transformation:

In this the similar grouped data gets de-transformed to obtain the clear denoised medical image as shown in Figure 9.

Fig. 9: Spectral De-transformation

3.2 Segmentation Phase:

In this stage, regions are segmented from the denoised CT image by using K-means clustering algorithm. K-means clustering segments the concerned CT image into two specific regions. The former region consists of the normal cells whereas the second region is composed of the tumourous cells. K-means clustering segments the CT image based on the intensity of pixels constituting the image. K-means is one of the most significant unsupervised learning algorithms with respect to clusters. Clustering means, grouping of pixels based on their characteristics. Here the image is clustered into *k* number of clusters. K-means clustering categorizes by minimizing the sum of squares of distances between data and the corresponding centroid of the cluster (A.K Jain, 2010; R. Chitta and M.N Murty, 2010). Here, K-means clustering groups the pixels into two distinct clusters *(k=2)*.The detailed step-by-steps of K-means clustering algorithm is presented as follows:

1) Give the number of cluster value as k . Here, we have assumed as, $k = 2$.
2) Randomly choose the k cluster centers.
3) Calculate mean or center of the cluster.

$$M = \frac{\sum x_i}{\frac{i:c(i)=k}{N_k}}, k = 1,2,..K \quad (5)$$

4) Next the pixels of the image are assigned to the closest cluster which satisfies the minimum Euclidean distance from the pixels values to the center of each cluster.

$$D(i) = \arg\max \left\| x_i - M_k \right\|^2, i = 1,...,K \quad (6)$$

5) If the distance is near to the center, then move to that cluster.
6) Else move to the next cluster.
7) Re-estimate the center.
8) Repeat the process until the center doesn't move further.

3.3 Feature Extraction Phase:

After we have achieved success in extracting the region, the recognition is carried out by means of feature extraction and classification technique to categorize it as either normal or tumour. Feature extraction computes the characteristics of an image to describe its texture properties. Here some features for the classification of tumour images are being considered.

$$FV = \{F_1, F_2, F_3\} \quad (7)$$

These features are calculated for the two segmented regions in each CT as tumour and non-tumour and the feature vector which is formulated as,

$$FV = \left\{F_1^T, F_1^{NT}, F_2^T, F_2^{NT}, F_3^T, F_3^{NT}\right\} \tag{8}$$

Where,

F_1^T → Contrast feature set of tumour region

F_1^{NT} → Contrast feature set of Non-tumour region

F_2^T → Energy feature set of tumour region

F_2^{NT} → Energy feature set of Non-tumour region

F_3^T → Entropy feature set of tumour region

F_3^{NT} → Entropy feature set of Non-tumour region

The feature vector FV is computed based on the features:

- ***Contrast*:**

The contrast (C) feature is defined as the divergence moment of the P matrix and constitutes a significant measure of the contrast. It is the amount of local variations present in an image. The formula for the estimation of the contrast is given below:

$$F_1 = C = \sum_{i=0}^{G-1}\sum_{j=0}^{G-1}(i-j)^2 p(i,j) \tag{9}$$

- ***Energy*:**

Energy (E) is employed to express a measure of information in an image. The formula for determination of the energy is as follows:

$$F_2 = E = \sum_{i=0}^{G-1}\sum_{j=0}^{G-1}[p(i,j)]^2 \tag{10}$$

- ***Entropy***:

An entropy (H) measure is a significant statistical measure of randomness which is employed to distinguish the texture inherent in the candidate region. The formula to compute entropy is as given below:

$$F_3 = H = -\sum_{i=0}^{G-1}\sum_{j=0}^{G-1} p(i,j)\log_2[p(i,j)] \tag{11}$$

The extracted features to a cuckoo based neuro-fuzzy classifier to accomplish the classification process.

3.4 Classification by CNF:

In this phase, the extracted feature set $FV = \left\{F_1^T, F_1^{NT}, F_2^T, F_2^{NT}, F_3^T, F_3^{NT}\right\}$ is given to the CNF classifier. In the CNF classifier, cuckoo search algorithm is employed for training the neural network and the fuzzy rules are generated according to the weights of the training sets. Then, classification is done based on the fuzzy rules generated. Section 3.4.1 describes best rule generation process using cuckoo search algorithm. Section 3.4.2 describes classification using neuro-fuzzy classifier.

3.4.1 Best rule generation using Cuckoo Search:

Cuckoo search algorithm is utilized to generate the best rule and this best rule is given for further processing (X.S Yang and S. Deb, 2009; E. Valian *et al.*, 2011). The detailed process of the generating the best rules using cuckoo search algorithm is explained as follows,

- ***Discretization:***

Initially, before the cuckoo search process, the training dataset DS_{TR}, which consists of $"N"$ number of attributes, is provided to the discretization function to relocate the input records into a discretized one. The generalization form of the training dataset is expressed by,

$$DS_{TR} = \left\{ds_{ij}; 0 \le k \le m \; and \; 0 \le l \le n\right\} \tag{12}$$

Australian Journal of Basic and Applied Sciences, 8(18) December 2014, Pages: 335-349

Discretization is an important step in data processing to transform the records with a specific interval. The utmost and least values of each and every attribute are located and the T interval is traced by consideration the relation between the deviated value and T^{th} value.

For each and every l , the deviated value is calculated as follows:

$$Dev_l = \frac{Max(ds_l) - \min(ds_l)}{4} \tag{13}$$

$$DS_l^{VL} = \min(ds_l) \le (\min(ds_l) + Dev_l) \tag{14}$$

$$DS_l^{L} = (\min(ds_l) + Dev_l) \le (\min(ds_l) + 2 * Dev_l) \tag{15}$$

$$DS_l^{M} = (\min(ds_l) + 2 * Dev_l) \le (\min(ds_l) + 3 * Dev_l) \tag{16}$$

$$DS_l^{H} = (\min(ds_l) + 3 * Dev_l) \le \max(ds_l)_l \tag{17}$$

Where,

$VL \rightarrow$ Very High, $H \rightarrow$ High,

$M \rightarrow$ Medium, $L \rightarrow$ Low

Then, every value that comes within the range is replaced with the interval value so that the input data is transformed to the discretized data DS_{TR} . After discretization function, the training dataset DS_{TR} is converted into discretized format DS_D . Where, the entire data element $DS_D(k,l)$ contain only the VL, L, M or H if $T = 4$.

- ***Generating initial set of nests:***

Initially, 'n' number of nests are engendered and each and every nest is broadly detailed as Very High (VL), High (H), Medium (M), Low (L) and one class (C). Here C corresponds to class (whether tumour or non-tumour). The population of nest 'n' is supplied to the client along with the dimension (attributes) of the each and every nest $R_i(f_i, C)$ forming part of the image feature dataset. In other words, 'n' solutions are furnished in a preliminary group of host nests, and each and every nest stands for the corresponding features. Where, f_i is the number of features, in which 1 represents Very High (VL), 2 represents High (H), 3 represents Medium (M), 4 represents Low (L) and $C \rightarrow$class. The initial solution and solution encoding process is depicted in Figure 10.

Fig. 10: Solution encoding process

- ***Fitness calculation:***

We compare the outcome result with the training and testing dataset and we calculate the accuracy through the following equation (18), as fitness function for each nest.

$$Fitness = sum\ \ of\ rule\ R_i\ \ \ in\ \ \ the\ \ \text{discretized}\ \ dataset\ DS_D \tag{18}$$

Where,

$DS_D \rightarrow$ discretized format data

R_i → Rules

- ***Nest updation:***

At this point, an arbitrary number (j) is created by using levy flight and the comparative remedy is chosen. Subsequently, the fitness of nest located in the initial group of nest corresponding to the arbitrary number is replaced by means of a new finest nest. When the estimation of the fitness of the initial remedies is over, newest remedy is found out in accordance with the cuckoo operator. Based on the modifiable Levy flight, the cuckoo operator generates new remedies. A new remedy $x^{(t+1)}$ for cuckoo i is produced by employing a Levy flight along with the following equation:

$$x^{(t+1)} = x_i^{(t)} + \alpha^{Levy(\lambda)} \tag{19}$$

Where, α $(\alpha > 0)$ symbolizes a step scaling size. This parameter must be connected to the scales of issue the algorithm is trying to locate a key to. In almost all the cases α can be fixed to the value of 1 or a specific dissimilar constant.

***Best rule generation*:**

From cuckoo search algorithm, logical rules, represented as $R = \{R_j; 1 \le j \le m\}$ are derived by performing several iterations. Here, the rules should have two different decisions such as, 1 and 2. From the cuckoo search algorithm, best rules R_{best} are generated and given as Figure 11.

Feature						C
2	2	2	2	2	2	1

Feature						C
2	2	2	2	2	2	2

Feature						C
1	1	1	1	1	1	1

Fig.11: Best rules from Cuckoo Search algorithm

3.4.2 Classification using Neuro-Fuzzy:

Generation of fuzzy score using fuzzy system:

The NF Classifier is a multi-layer feed forward network which comprises the ensuing levels. The fuzzy interference system performs three dynamic functions as listed below:

- Fuzzification
- Rule Evaluation
- Defuzzification

Fuzzy inference is the unique procedure of generating a mapping from a prearranged input to the resultant output by the employment of a fuzzy logic. Thereafter, the mapping heralds a foundation and from this foundation appropriate decisions can be taken, and the patterns can be distinguished. The key task of fuzzy inference involves Membership Functions, Logical Operations, and If-Then Rules. The schematic graph of the fuzzy inference system (FIS) is vividly illustrated in Figure 12.

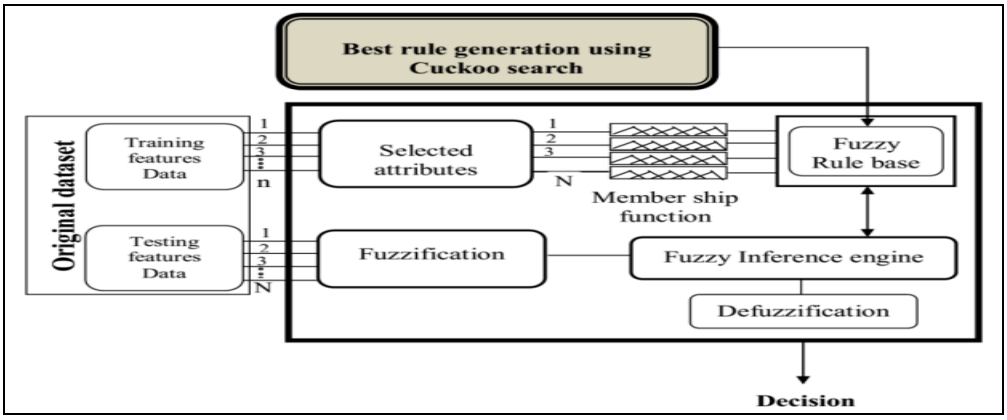

Fig.12: Fuzzy Inference System Structure

- ***Fuzzification:***

In fuzzification process, the crusty quantities are changed into fuzzy. In our proposed method, the fuzzification process is carried out by employing the features that are extracted in section 4.2.3. The extracted features are $F_1^T, F_1^{NT}, F_2^T, F_2^{NT}, F_3^T \; and \; F_3^{NT}$, for each feature we perform fuzzification process. For the fuzzification process, we collect all the $F_1^T, F_1^{NT}, F_2^T, F_2^{NT}, F_3^T \; and \; F_3^{NT}$ features of the training images and compute each feature minimum (min) and maximum (max) values. The fuzzification process is performed by the following equations.

$$[FL_1^T]^{Min\,Limit} = \min + \left(\frac{\max - \min}{3}\right) \tag{20}$$

$$[FL_1^T]^{Max\,Limit} = Max\,Limt + \left(\frac{\max - \min}{3}\right) \tag{21}$$

In the above equations $[FL_1^T]^{Min\,Limit}$ and $[FL_1^T]^{Max\,Limit}$ are the minimum and maximum limit values of the feature F_1^T. The same equations are used for the features $F_1^T, F_1^{NT}, F_2^T, F_2^{NT}, F_3^T \; and \; F_3^{NT}$ to compute the minimum and maximum limit values.

- ***Fuzzy Membership function:***

The membership function of each and every input is recognized in this stage. The membership function is planned by selecting the appropriate membership function. One of the prominent challenges in all fuzzy sets involves the appropriate decision of fuzzy membership functions,

1) The membership function discharges its task efficiently by performing the complete demarcation of the fuzzy set.
2) A membership function furnishes an assessment tool for estimating the level of resemblance of an element to a fuzzy set.
3) Membership functions may assume any shape; however there occur certain general patterns which tend to emerge in bona fide applications.

- ***Rule Evaluation:***

Using cuckoo search algorithm, we already generated the fuzzy rule set $R_{best} = \{R^j{}_{best}; 1 \le j \le m - T,\}$ that are given in the fuzzy rule base. The rule base contains a set of fuzzy rules.

***Neural network process*:**

After the fuzzy interference process, the fuzzy score is generated and assigned to the neural network output parameter. Totally, we have assigned two output classes (parameter), (i) fuzzy score (ii) original feature set. The neural network is well trained with these extracted features and different numbers of unknown CT images are tested. The important steps involved in neural network are shown in Figure 13, as follows,

Step 1: Put the input weights to every neuron except the neurons in the input layer. Here, $F_1^T, F_1^{NT}, F_2^T, F_2^{NT}, F_3^T \; and \; F_3^{NT}$ are the input features such as contrast, energy, entropy for the tumour and non-tumour segmented region i.e. input of the network and $(C_k)output$ is the decision result from the FIS and original feature set, i.e. output of the network.

Step 2: The neural network is designed with six input layers, H_i hidden layer, and two output layer. The weights and then added to the neural network and it is biased.

Step 3: To the output layer the output of the activation function $f(\ln(H_i))$ is then broadcast all of the neurons:

$$(C_l)output = \eta_k + \sum_{n=1}^{N} W_{2nl} C_l(n) \tag{22}$$

Where η_i and η_k are the biases in the hidden layer and the output layer.

Step 4: Compute the error between the desired output $(C_k)_{Target}$ and the output $(C_k)_{output}$ produced by the feed-forward neural network, this is given by,

$$E_v = (C_k)t\arg et - (C_k)output \tag{23}$$

In equation (23) $(C_k)_{target}$ is the target output and $(C_k)_{output}$ is the network output.

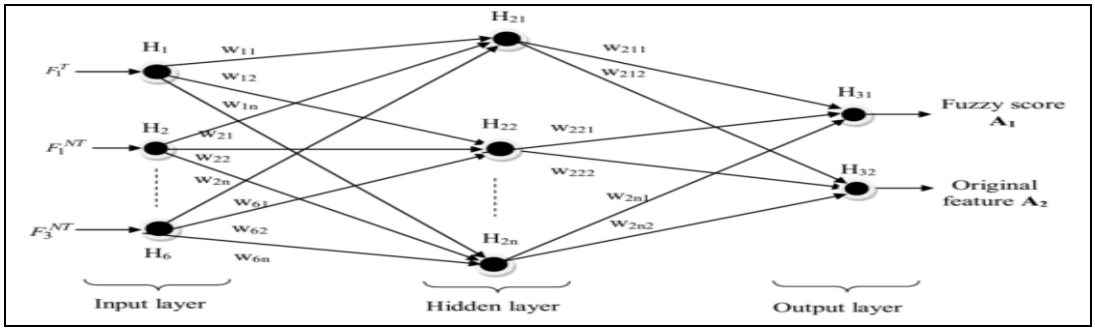

Fig. 13: Proposed Neural Network Structure

In testing phase, the input testing feature $[F_1, F_2, F_3]_{test}$ is given to fuzzy interference system and corresponding fuzzy score is generated. This fuzzy score is given to the neural network. The resultant value of neural network's output class is represented as A_1 and A_2 , and this value is compared with threshold value T_1 .

$$\text{Re}\,sult = \begin{cases} Abnormal; A_1 \geq T_1 \\ Normal; A_2 \leq T_1 \end{cases} \quad (24)$$

In this way the CT images are classified as normal and abnormal.

4. Implementation Methodology:

This section presents the details about the simulation environment and the evaluation metrics are being discussed. The proposed approach of image denoising is experimented with the CT medical images and the result is evaluated with the PSNR and SDME. The obtained denoised image is then evaluated for the parameters sensitivity, specificity and accuracy for estimating the correctness of the image.

4.1 Simulation Environment:

The proposed method is implemented in a Windows machine having a configuration of Intel (R) core I5 processor, 3.20 Ghz, 4 GB RAM and the operation system platform Is Microsoft Windows7 Professional. We have used Matlab latest version (7.12) for this proposed technique.

4.2 Evaluation Metrics:

The formulae used to compute the evaluation metrics PSNR, SDME, sensitivity, specificity and accuracy values are given as follows.

4.2.1 Peak Signal to Noise Ratio (PSNR):

The formula for PSNR value computation is (A.Velayudham *et al.*, 2013),

$$PSNR = 10\log_{10}\frac{E_{\max}^2 \times I_w \times I_h}{\sum\left(I_{xy} - I_{xy}^*\right)}$$

Where, I_w and I_h → Width and height of the denoised image

I_{xy} → Original image pixel value at coordinate (x, y)

I_{xy}^* → Denoised image pixel value at coordinate (x, y)

$E_{\max}^2$ → Largest energy of the image pixels

4.2.2 Second Derivative Measure of Enhancement (SDME):

The formula for SDME value computation is given by (Karen Panetta *et al.*, 2011),

$$SDME = -\frac{1}{k_1 k_2} 20\ln\left|\frac{I_{\max;k,l} - 2I_{center,k,l} + I_{\min;k,l}}{I_{\max;k,l} + 2I_{center,k,l} + I_{\min;k,l}}\right|$$

Where the denoised image is divided into ($k_1 \times k_2$) blocks with odd size, $I_{\max;k,l}$ and $I_{\min;k,l}$ correspond to the maximum and minimum values of pixels in each block whereas $I_{center;k,l}$ is the value of the intensity of the pixel in the center of each block.

4.2.3 Sensitivity, Specificity and Accuracy:

The evaluation of proposed technique in different CT images are carried out using the following metrics as suggested by below equations,

$$\text{Sensitivity} = \frac{No.of\ true positives}{No.of\ true positives + No.of\ false negatives}$$

$$\text{Specificity} = \frac{No.of\ true negatives}{No.of\ true negatives + No.of\ false positives}$$

$$\text{Accuracy} = \frac{No.of\ true positives + number of\ true negatives}{No.of\ true positives + false negatives + true negatives + false positives}$$

RESULTS AND DISCUSSION

In Table 1, the proposed technique is compared with the existing technique (Sachin D. Ruikar, 2011).

Table 1: Comparison Table Of Proposed With Existing Technique (Sachin D. Ruikar, 2011)

Input CT images	Proposed Denoised CT images	Noise	Variance level	Proposed Technique		Existing (Sachin D. Ruikar , 2011)	
				PSNR	SDME	PSNR	SDME
		Gaussian	0.02	21.1287	46.7269	16.7166	43.7036
			0.04	19.6213	44.338	14.7828	37.9114
			0.06	18.646	43.9474	13.5612	34.4204
		Salt & Pepper	0.02	25.1008	69.8798	21.634	52.0768
			0.04	25.0776	64.9669	18.567	46.527
			0.06	20.4357	43.101	17.0057	38.0931
		Gaussian	0.02	21.3186	48.9719	16.8026	45.1277
			0.04	19.9728	47.3975	14.8172	38.9988
			0.06	18.6979	46.162	13.6043	35.6109
		Salt & Pepper	0.02	29.841	67.5065	21.8661	52.9996
			0.04	21.7599	65.2206	18.918	49.4154
			0.06	20.5562	44.0129	16.9189	38.2141
		Gaussian	0.02	21.206	48.2659	16.7567	45.1306
			0.04	19.9561	48.3279	14.8153	39.8488
			0.06	18.828	47.5855	13.5965	35.9237
		Salt & Pepper	0.02	22.5698	67.9266	21.7306	63.3859
			0.04	21.2678	64.7767	18.8978	49.0446
			0.06	20.5852	43.7783	17.0635	39.7519
		Gaussian	0.02	21.3496	49.7599	16.7834	45.4059
			0.04	19.9989	46.7261	14.856	39.5777
			0.06	18.9786	46.0037	13.5704	36.3572
		Salt & Pepper	0.02	22.1813	64.3396	21.8897	54.1842
			0.04	21.4148	68.8235	18.7489	48.8421
			0.06	20.8899	43.8492	17.0178	38.2939
		Gaussian	0.02	21.1233	47.992	16.7386	43.3181
			0.04	19.8723	46.4375	14.8244	37.8772
			0.06	18.8407	44.4947	13.5808	34.7142
		Salt & Pepper	0.02	21.7314	65.8095	21.4638	50.4402
			0.04	21.1082	63.1082	18.9884	49.5018
			0.06	19.9906	42.0401	16.9854	38.365

In this paper, we have compared our proposed denoising technique against existing technique (D. Sachin Ruikar, 2011) with five CT images. The performance analysis has been made for the evaluation metrics such as PSNR and SDME. By analyzing the evaluation metrics, the performance of the proposed technique has significantly improved the PSNR and SDME values. Totally, from Table 1, the proposed denoising technique has achieved better results when compared with the existing technique (D. Sachin Ruikar, 2011). Table 2 shows the results after the extraction of features taking into consideration the parameters contrast, energy and entropy. The evaluation results of the proposed against existing technique have shown better outcomes.

Sensitivity, Specificity and Accuracy graphs are shown in Figure 14 to 16. In Figure 14, the proposed approach achieved the sensitivity of about 96.9% whereas the existing approach achieved only 8.7% in training-

testing ratio (70-30). In Figure 15, the proposed technique achieved the specificity of 78.89% whereas the existing approach achieved only 72.27% in training-testing ratio (80-20). In Figure 16, the proposed approach achieved the accuracy of about 79.809% whereas the existing approach achieved only 76.92% in training-testing ratio (90-10). Totally, the proposed tumour detection technique has obtained better performance evaluation when compared to the existing technique.

Table 2: Output parameters after feature extraction

Input CT Images	Proposed Denoised CT Images	Contrast	Energy	Entropy
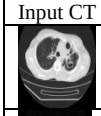		0.8095	653456	1.2239
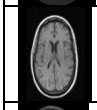	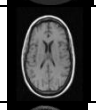	0.7089	945342	1.4876
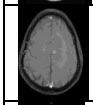	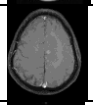	0.6881	832579	1.1567
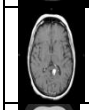	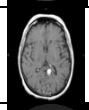	0.7883	710543	1.2765
		0.8765	599876	1.2314

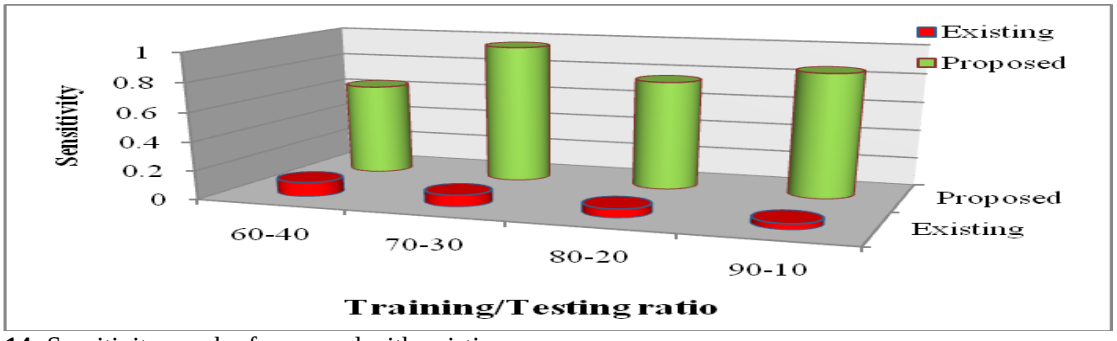

Fig. 14: Sensitivity graph of proposed with existing

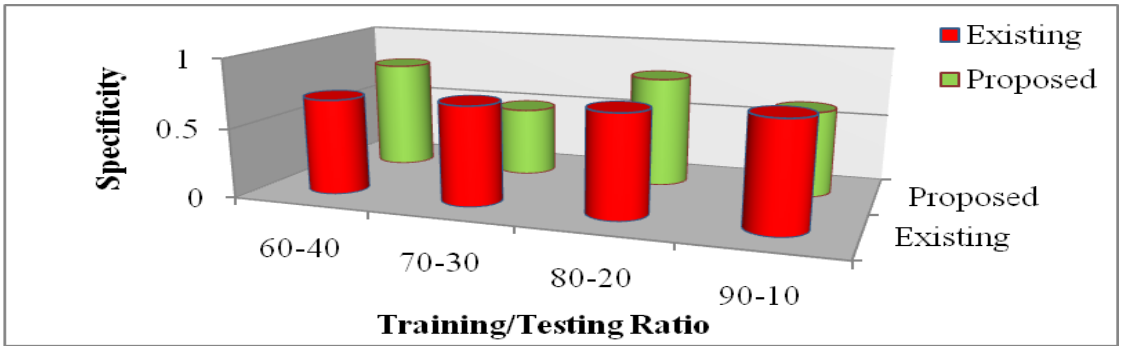

Fig. 15: Specificity graph of proposed with existing

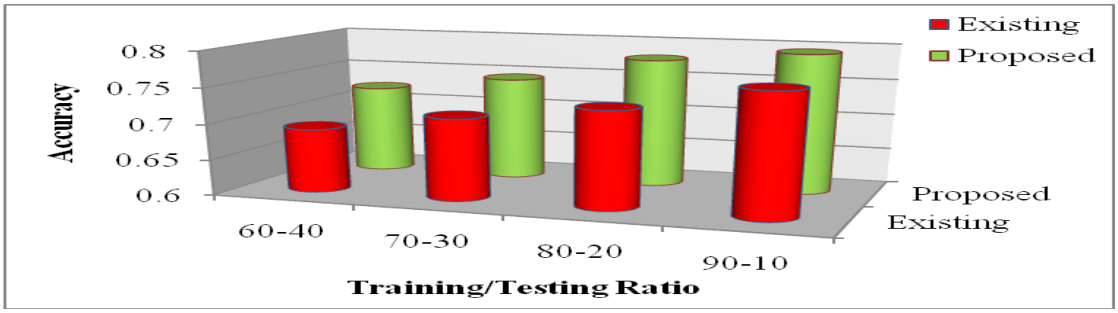

Fig. 16: Accuracy graph of proposed with existing

Conclusion:

In this paper, we have provided a methodology for medical image denoising and a classification technique using Non-local denoising, based on ML Estimation approach and Cuckoo-Neuro Fuzzy classifier. In this paper a framework was presented to optimize the performance of medical images taking into consideration two noises, Gaussian and salt & pepper, evaluating the noise levels on five CT images for the parameters PSNR and SDME. For comparison analysis, our proposed denoising technique is compared with the existing work in various noise levels. Our obtained outcomes have confirmed that the proposed denoising technique have shown better values for the SDME of 69.8798 and PSNR of 25.1008 for salt & pepper noise which is very superior and very effective, compared to existing methods. Moreover its performance was evaluated qualitatively and it has shown an accuracy of 96.9% towards tumour detection, which is much better when compared to existing methods.

REFERENCES

Abdolhossein Fathi and Ahmad Reza Naghsh-Nilchi, 2012. “Efficient Image Denoising Method Based on a New Adaptive Wavelet Packet Thresholding Function”, IEEE Transactions on Image Processing, 21(9): 3981-3990.

Anja Borsdorf, Rainer Raupach, Thomas Flohr and Joachim Hornegger, 2008. “Wavelet based Noise Reduction in CT-Images using Correlation Analysis”, IEEE transactions on Medical Imaging, 27(12): 1685-1703.

Arcan Erturk, M., Paul A. Bottomley and AbdEl-Monem M. El-Sharkawy, 2013. “Denoising MRI Using Spectral Subtraction”, IEEE Transactions On Biomedical Engineering, 60(6): 1556-1562.

Buades, A., B. Coll and J. M. Morel, 2005. “A non-local algorithm for image denoising”, in Proc. IEEE Comput. Soc. Conf. Comput. Vis. Pattern Recognition, 2: 60-65.

Chen, G.Y and B. Kegl, 2007. “Image denoising with complex ridgelets”, Pattern Recognition, 40: 578-585.

Chitta, R. and M. N. Murty, 2010. “Two-level K-means clustering algorithm for k-τ relationship establishment and linear-time classification”, Pattern Recognition, 43(3): 796-804.

Ehsan Nadernejad and Mohsen Nikpour, 2012. "Image denoising using new pixon representation based on fuzzy filtering and partial differential equations”, Digital Signal Processing, 22: 913-922.

Faten Ben Arfia, Mohamed Ben Messaoud and Mohamed Abid, 2010. “A New Image denoising Technique combining the Empirical Mode Decomposition with a Wavelet Transform Technique”, 17th International Conference on Systems, Signals and Image Processing, 514-517.

Gerig, G., O. Kubler, R. Kikinis, and F.A. Jolesz, 1992. “Nonlinear anisotropic filtering of MRI data”, IEEE Trans. Medical Imaging, 11(2): 221-232.

Guangming Zhang, Zhiming Cui, Jianming Chen and Jian Wu, 2010. "CT Image De-noising Model Based on Independent Component Analysis and Curvelet Transform”, Journal of Software, 5(9): 1006-1013.

Jain, A.K, 2010. “Data clustering: 50 years beyond K-means”, Pattern Recognition Letters, 31(8): 651-666.

Jeny Rajan, Ben Jeurissen, Marleen Verhoye, Johan Van Audekerke and Jan Sijibers, 2011. “Maximum likelihood estimation –based denoising of magnetic resonance images using restricted local neighborhoods”, Physics in Medicine and Biology, 56: 5221-5234.

Jeny Rajan, Johan van Audekerke, Annemie Van der Linden, Marleen Verhoye and Jan Sijbers, 2012 “An adaptive nonlocal maximum likelihood estimation method for denoising magnetic resonance images”, IEEE, 12.

Jitendra Malik, Serge Belongie, Thomas Leung and Jianbo Shi, 2001. “Contour and Texture Analysis for Image Segmentation”, International Journal of Computer Vision, 43(1): 7-27.

Joao M. Sanches, Jacinto C. Nascimento and Jorge S. Marques, 2008. “Medical Image Noise Reduction using the Sylvester–Lyapunov Equation”, IEEE Transactions On Image Processing, 17(9): 1522-1539.

Jue Wu and Albert C.S Chung, 2009. “A novel framework for segmentation of deep brain structures based on Markov dependence tree”, NeuroImage, 46: 1027-1036.

Karen Panetta, Yicong Zhou, Sos Agaian and Hongwei Jia, 2011. "Nonlinear Unsharp Masking for Mammogram Enhancement”, IEEE Transactions On Information Technology In Biomedicine, 15(6): 918-928.

Kekre, H.B. and Ms. Saylee M. Gharge, 2010. “Image Segmentation using Extended Edge Operator for Mammographic Images”, International Journal on Computer Science and Engineering, 2(4): 1086-1091.

Landi, G. and E.Loli Piccolomini, 2012. "An efficient method for nonnegatively constrained Total Variation-based denoising of medical images corrupted by Poisson noise," Computerized Medical Imaging and Graphics , 36: 38-46.

Manjon, J.V., P. Coupe, L. Marti-Bonmati, D. L. Collins, and M. Robles, 2010. “Adaptive non-local means denoising of MR images with spatially varying noise levels”, J. Magn. Resonance Imag., 31(1): 192-203.

Minakshi Sharma and Dr. Sourabh Mukharjee, 2012. “Brain Tumour Segmentation using hybrid Genetic Algorithm and Artificial Neural Network Fuzzy Inference System (ANFIS)”, International Journal of Fuzzy Logic Systems, 2(4): 31-42.

Naga Prudhvi Raj, V. and Dr T Venkateswarlu, 2012. "Denoising of medical images using dual tree complex wavelet transform", Procedia Technology, 4: 238-244.

Nowak, R.D., 1999. "Wavelet-based rician noise removal for magnetic resonance imaging", IEEE Trans. Image Process., 8(10): 1408-1419.

Orchard, J., M. Ebrahimi, and A. Wong, 2008. "Efficient nonlocal-means denoising using the SVD," in Proc. 15th IEEE Int. Conf. Image Process., 1(5): 1732-1735.

Perona, P. and J.Malik, 1990. "Scale-space and edge-detection using anisotropic diffusion", IEEE Trans. Pattern Anal.Mach. Intell., 12(7): 629-639.

Qin, A.K. and David A. Clausi, 2010. "Multivariate Image Segmentation Using Semantic Region Growing with Adaptive Edge Penalty", Image processing-IEEE Transaction, 19(8): 2157-2170.

Rakesh, M. and T. Ravi, 2012. "Image Segmentation and Detection of Tumor Objects in MR Brain Images Using Fuzzy C-Means (FCM) Algorithm", International Journal of Engineering Research and Applications, 2(3): 2088-2094.

Reza Farjam, Hemant A. Parmar, Douglas C. Noll, Christina I. Tsien and Yue Cao, 2012. " An approach for computer-aided detection of brain metastases in post-Gd T1-W MRI", Magnetic Resonance Imaging, 30(6): 824-836.

Sachin D. Ruikar and Dharmpal D Doye, 2011. "Wavelet Based Image Denoising Technique", International Journal of Advanced Computer Science and Applications, 2(3): 49-53.

Savitharaj, N.S., A.Velayudham and Dr.R.Kanthavel, 2014. "An adaptive framework for non-local MRI denoising based on ML estimation approach using regularizers", International Journal of Engineering and Innovative Technology, 3(9):123–127.

Shanshan Wang, Yong Xia, Qiegen Liu, Jianhua Luo, Yuemin Zhu and David Dagan Feng, 2012. "Gabor feature based nonlocal means filter for textured image denoising", J. Vis. Commun. Image R., 23: 1008-1018.

Shutao Li, Leyuan Fang and Haitao Yin, 2012. "An Efficient Dictionary Learning Algorithm and Its Application to 3-D Medical Image Denoising", IEEE Transactions on Biomedical Engineering, 59(2): 417-427.

Sijbers, J., A. J. Den Dekker, J. Van Audekerke, M. Verhoye, and D. Van Dyck, 1998. "Estimation of the noise in magnitude MR images", Magn. Resonance Imag., 16(1): 87-90.

Sudipta Roy, Nidul Sinha, Asoke K. Sen, 2010. "A New Hybrid Image Denoising Method", International Journal of Information Technology and Knowledge Management, 2(2): 491 - 497.

Syed Amjad Ali, Srinivasan Vathsal and K. Lal Kishore, 2010. "An Efficient Denoising Technique for CT Images using Window-based Multi-Wavelet Transformation and Thresholding", European Journal of Scientific Research, 48(2): 315-325.

Tao Wang, I. Cheng and Basu, 2009. "Fluid Vector Flow and Applications in Brain Tumor Segmentation", Biomedical Engineering-IEEE Transactions, 56(3): 781-789.

Tischenko, O., C. Hoeschen and E. Buhr, 2005. "An artifact-free structure saving noise reduction using the correlation between two images for threshold determination in the wavelet domain", Medical Imaging 2005: Image Processing- Proceedings of the SPIE., J. M. Fitzpatrick and J. M. Reinhardt, Eds., 5747: 1066-1075.

Valian, E., S. Mohanna and S. Tavakoli, 2011. "Improved Cuckoo Search Algorithm for Global Optimization", International Journal of Communications and Information Technology (IJCIT), 1(1): 31-44.

Velayudham, A. and R.Kanthavel, 2013. "An Efficient Approach for Denoising of CT-Images Using EMD and Dual Tree Complex Wavelet Packets", International Review on Computers and Software, 8(9): 2088-2101.

Yang, X.S, and S. Deb, 2009. "Cuckoo search via Levy flights", in: Proc. of World Congress on Nature & Biologically Inspired Computing (NaBIC2009), IEEE Publications, 210-214.

Zafer Iscan, Zumray Dokur and Tamer Olmez, 2010. "Tumor detection by using Zernike moments on segmented magnetic resonance brain images", Expert Systems with Applications, 37(3): 2540-2549.